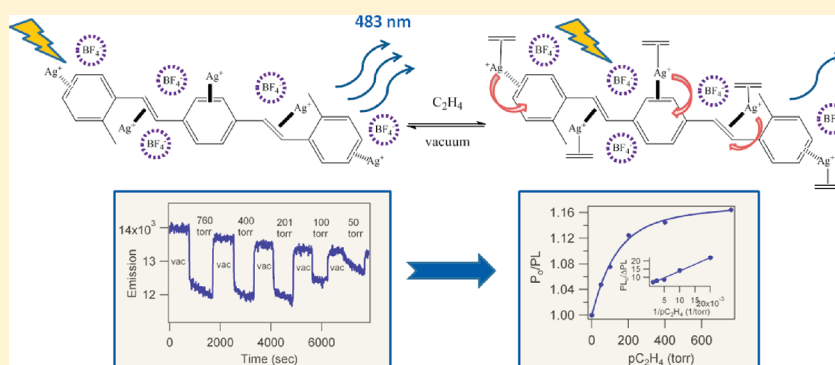


## Ethylene Sensing by Silver(I) Salt-Impregnated Luminescent Films

Michael Santiago Cintrón,<sup>‡</sup> Omar Green, and Judith N. Burstyn\*

Department of Chemistry, University of Wisconsin, Madison, Wisconsin 53706, United States

## S Supporting Information



**ABSTRACT:** Luminescent oligomers and polymers doped with silver(I) salts were used as optical sensors for ethylene and other gaseous small molecules. Films of poly(vinylphenylketone) (PVPK) or 1,4-bis(methylstyryl)benzene (BMSB) impregnated with AgBF<sub>4</sub>, AgSbF<sub>6</sub>, or AgB(C<sub>6</sub>F<sub>5</sub>)<sub>4</sub> respond to ethylene exposures with a reversible emission quenching that is proportional to the pressure of the gas. Experiments with various analytes revealed that only gases capable of forming coordinate bonds with Ag(I) ions (i.e., ethylene, propylene, and ammonia) produced a sensing response. Comparison of the effects of ethylene and tetradeuterioethylene revealed that the emission quenching was due to enhanced vibrational relaxation. The Ag(I) ions are essential to the observed optical response. The oligomer/polymer support enhances the response characteristics of the impregnated salt by promoting separation of Ag(I) from its anion, a separation that improves accessibility of the Ag(I) ion to the gaseous analytes. Salts with large lattice energies, where the anion is not dissociated from Ag(I) in the matrix, fail to sensitize film responses. Photoluminescence experiments with Ag(I)-impregnated BMSB films established that the Ag(I) ions serve to communicate the analyte-binding signal to the support by altering the support-based emission. These experiments demonstrate a sensing paradigm where simultaneous coordination of Ag(I) ions to the support matrix and to a gaseous analyte enables the optical response.

## ■ INTRODUCTION

Ethylene is a gaseous hormone that regulates development in plants.<sup>1</sup> Produced by plants as they mature, ethylene permeates cells and binds to copper-containing receptor proteins.<sup>2–4</sup> Ethylene binding initiates growth responses that lead to plant maturation, flowering, fruiting, and eventually senescence.<sup>1</sup> Through its effects as a growth regulator, ethylene plays an important role in the postharvest stability of many fruits and vegetables. Although modern agricultural methods aim to temporarily suppress the physiological effects of ethylene<sup>5–7</sup> and to control ethylene accumulation during storage,<sup>1</sup> the agricultural industry suffers millions of dollars in annual losses due to premature rotting of produce exposed to the hormone.<sup>8</sup> Modern storage facilities control temperature, humidity, and oxygen levels through continuous monitoring and regulation, greatly increasing market lifetime.<sup>1</sup> Unfortunately, there are no cost-effective methods available to control ethylene levels. Current ethylene sensing technologies include tin oxide semiconductors,<sup>9</sup> photoacoustic spectroscopy,<sup>10</sup> and gas chromatography;<sup>11</sup> however, these technologies are bulky and expensive and do not provide real-time monitoring of ethylene levels.

A portable and inexpensive ethylene sensor could be used to monitor concentrations of the gaseous hormone and, combined with already existing ethylene removal technologies,<sup>12</sup> maintain optimal produce storage conditions. Toward this end, two sensing paradigms that combine the optical properties of luminescent polymers with the olefin-binding capability of coinage metal salts were recently described. In one technology, developed by Esser and Swager,<sup>13</sup> the fluorescence of a conjugated polymer was quenched by ethylene interaction with a Cu(I) complex. Exposure to ethylene disrupted the polymer/Cu(I) complex interaction and restored polymer emission. This fluorescence turn-on response enabled ethylene sensing in solution and in films. A second technology developed by our group and further explored herein uses silver(I)-impregnated polymer films as optical sensors for ethylene and other small gaseous molecules.<sup>14</sup> This sensing method builds on facilitated olefin transport technologies used to separate gaseous olefin

Received: December 30, 2010

Published: February 22, 2012

(unsaturated hydrocarbons) from paraffins (saturated hydrocarbons) in petroleum feedstreams.

In facilitated transport, carrier centers selectively and reversibly bind gas molecules of interest in a mixture increasing the gas solubility and providing a selective transport pathway through the separation medium.<sup>15</sup> Hemoglobin,<sup>16</sup> carbonate,<sup>17</sup> silver,<sup>18,19</sup> copper,<sup>20,21</sup> and ammonium salts<sup>22</sup> have been used as carriers in facilitated transport membranes. Among the gases transported are dioxygen, carbon dioxide, and low molecular weight alkenes (olefins). In the context of facilitated olefin transport, silver(I) salts are the most commonly used carrier.<sup>15</sup> While early olefin transport studies focused on supported liquid membranes<sup>23</sup> and ion-exchange membranes,<sup>19,24</sup> recent studies employ solid polymer membranes that function without a liquid medium.<sup>25</sup> These membranes typically contain ether or carbonyl functionalities that induce ion-pair separation in the carrier silver(I) salts, which aids in olefin–metal ion interaction.<sup>26</sup> Transport membranes can enrich, in an energy-efficient manner, olefin–paraffin (alkene–alkane) gas streams with selectivity of close to 250.<sup>27</sup>

A strategy parallel to that used to develop Ag(I)-impregnated facilitated transport membranes may be employed to design optical ethylene sensors. The approach relies on Ag(I) salts, which act as the active sensing sites, impregnated in a luminescent polymer, which plays an active role in priming the Ag(I) for sensing and transducing the response signal. We previously reported that AgBF<sub>4</sub>-impregnated poly(vinylphenylketone) (PVPK) films are effective for optical C<sub>2</sub>H<sub>4</sub> sensing.<sup>14</sup> Herein we describe the attributes of this sensing method, in which the polymer serves three roles: first as a support that promotes ion-pair separation to facilitate Ag(I) salt interaction with gaseous analytes, second as a matrix that maintains the viability of the Ag(I) centers during the sensing event, and third as a recipient of the ethylene binding signal.

## ■ EXPERIMENTAL SECTION

**Materials.** C<sub>2</sub>H<sub>4</sub>, C<sub>2</sub>D<sub>4</sub>, NH<sub>3</sub>, C<sub>3</sub>H<sub>6</sub>, C<sub>3</sub>H<sub>8</sub>, AgF, BF<sub>3</sub>·Et<sub>2</sub>O, poly(vinylphenylketone) (PVPK), polystyrene (PS), 1,4-bis-(methylstyryl)benzene (BMSB), and AgSbF<sub>6</sub> were purchased from Aldrich Chemical Co. (Milwaukee, WI). Sicapent drying agent was purchased from Fisher Scientific. Argon was purchased from Aga gas (99%), and house nitrogen gas was passed through a drying tube filled with Sicapent before use. AgBF<sub>4</sub> was purchased from Aldrich Chemical Co. or was prepared as described below. Spectroscopic grade solvents were purchased from Burdick and Jackson; tetrahydrofuran (THF) was distilled under N<sub>2</sub> from Na/benzophenone, and CH<sub>3</sub>CN was distilled under N<sub>2</sub> from CaH<sub>2</sub>.

**Synthesis of Silver Tetrafluoroborate (AgBF<sub>4</sub>).** AgBF<sub>4</sub> was synthesized by modification of a literature method.<sup>28</sup> BF<sub>3</sub>·Et<sub>2</sub>O (3 mL, 24.3 mmol) was added to a suspension of AgF (500 mg, 3.94 mmol) in 5 mL of Et<sub>2</sub>O. The suspension was stirred until a clear solution was obtained. Solvent and excess BF<sub>3</sub>·Et<sub>2</sub>O were removed *in vacuo* to obtain a crystalline white powder (650 mg., 89.7% yield). IR (powder): 765, 1065 cm<sup>-1</sup>.

**Synthesis of Silver Tetra(pentafluorophenyl)borate (AgB(C<sub>6</sub>F<sub>5</sub>)<sub>4</sub>).** AgB(C<sub>6</sub>F<sub>5</sub>)<sub>4</sub> was synthesized as reported.<sup>29</sup> An aqueous solution of AgNO<sub>3</sub> (500 mg, 2.94 mmol) in 10 mL of H<sub>2</sub>O was added to a solution of KB(C<sub>6</sub>F<sub>5</sub>)<sub>4</sub> (200 mg, 0.279 mmol) in 10 mL of Et<sub>2</sub>O. The biphasic mixture was stirred vigorously for 10 min. The layers were separated, the organic phase was dried with Na<sub>2</sub>SO<sub>4</sub>, and the ether was removed *in vacuo*; this procedure afforded a white crystalline powder (140 mg, 64% yield). IR (powder): 1650, 1517, 1462, 1376, 1272, 1090, 976, 774, 756, 684, 662 cm<sup>-1</sup>. ICP-AES analysis of AgB(C<sub>6</sub>F<sub>5</sub>)<sub>4</sub>, performed with a Perkin-Elmer Optima 2000 ICP-OES, revealed that there was less than 1% K in the product.

**Preparation of Metal Salt-Impregnated Films.** Films were prepared as previously described.<sup>14</sup> The selected polymer, PVPK or PS, and a metal salt were dissolved in THF or CH<sub>3</sub>CN to a final concentration of 0.05 M polymer repeating unit and 0.10 M silver salt. The solution (150 μL) was placed dropwise on a sliver of a Fisher brand microscope slide and allowed to air-dry. The sample slide was then mounted in a Schlenk luminescence cell and allowed to dry overnight *in vacuo*. The same method was used to prepare films of BMSB oligomer, with concentrations of 0.05 M oligomer and 0.25 M silver salt.

**IR Studies.** The experimental BMSB oligomer to silver salt ratio was determined by monitoring IR peaks associated with oligomer ring stretches. A THF solution (4 mL) of BMSB (40.0 mg, 0.129 mmol) was added to vials containing varying amounts of AgBF<sub>4</sub> (2–7 equiv where 1 equiv corresponds to 25.1 mg). The solution was mixed for 5 min and diluted to a total volume of 6 mL. Each solution (0.2 mL) was deposited onto a NaCl plate and allowed to air-dry for 15 min. The film-bearing NaCl plate was then placed in a Schlenk-style gas cell, designed for gas exchange. The samples were then dried under vacuum for an hour, and their FT-IR spectra were recorded in a Bruker Vertex 70 spectrometer. To probe analyte binding, a film of BMSB with 5 equiv of AgSbF<sub>6</sub> was similarly prepared. After vacuum drying, the film was exposed to a flow of CO for 15 min, followed by three Ar-purge and one-hour vacuum cycles. FT-IR spectra before and after CO exposure were collected. All reported spectra were recorded under vacuum with a spectral resolution of 4 cm<sup>-1</sup> and are shown as the average of 32 scans.

**Photoluminescence (PL) studies.** Films of PVPK, PS, and BMSB impregnated with varying ratios of Ag(I) salts were studied. A gas-flow apparatus comprised of a manifold and pressure gauge was used to control the pressures of gases to which the films were exposed. All connections were made with flexible steel tubing. Photoluminescence experiments were performed either as previously described<sup>14</sup> or by the modified method described below. Ag(I)-impregnated films of PS and PVPK required several conditioning cycles of alternating exposure to C<sub>2</sub>H<sub>4</sub> and vacuum to remove coordinated solvent molecules before they produced a consistent and reproducible quenching in response to C<sub>2</sub>H<sub>4</sub>. Data were collected after the film demonstrated three quenchings of equal intensity in response to 760 Torr C<sub>2</sub>H<sub>4</sub>. Films of PVPK and PS gave maximal response to ethylene with 2 equiv of AgBF<sub>4</sub> per monomer unit. Freshly prepared Ag(I)–BMSB films exhibited consistent quenching in response to C<sub>2</sub>H<sub>4</sub> following an single conditioning cycle. BMSB PL experiments were performed with films impregnated with 5 equiv of AgBF<sub>4</sub> per oligomer. For consistency, identical film conditioning procedures were used for all PL experiments, with PVPK, PS, and BMSB films exposed to three cycles of C<sub>2</sub>H<sub>4</sub> and vacuum prior to experimental data collection.

Changes in PL in response to gas exposure were recorded as a function of the intensity of the peak maximum in the emission spectrum with time. The PVPK and PS film samples were excited with 0.25–1.6 mW of 488 nm light from an Ar<sup>+</sup> ion laser (Coherent Innova 90). The emitted light was collected with an Oriel fiber optic attached to a Multispec CCD counter. Interference by incident laser light was eliminated with a high pass filter (Omega Optical), with a cutoff at 510 nm, in the CCD counter. Alternatively, PL runs were performed with a 300 W xenon arc lamp (Spectra Physics) equipped with a dichroic mirror (420–630 nm) and a fiber optic coupler. For experiments with BMSB, light output from the arc lamp was attenuated with a Schott BG-12 filter (Newport) that closely resembles the absorption profile of BMSB. Emission at 482 nm was monitored as above. Incident light interference was minimized by use of a high-pass filter (Omega Optical) centered at 460 nm. The output intensity of the BMSB films was attenuated using a neutral density filter (1/64; Omega Optical). Data points for all experiments were recorded every 8 s, and these points reflected the counts accumulated within the time interval. All data were collected by use of Instaspec for Windows (v. 1.21g) and analyzed with Microsoft Excel and Igor Pro (version 3.14). Complete emission spectra were collected at the beginning and end of each experiment; for each film, the emission profile was collected and the

emission maximum under vacuum determined. The change in emission intensity in response to different gas atmospheres was monitored at the emission maximum. Films were exposed to argon, ambient air,  $C_2H_4$ ,  $C_2D_4$ ,  $NH_3$ ,  $C_3H_6$ , or  $C_3H_8$  over a range of pressures. All analytes for which a response was observed caused a quenching in luminescence, and the data were analyzed by use of eq 1. Stern–Volmer and modified Stern–Volmer analysis were performed using equations found in ref 14.

$$\text{fractional quenching} = [PL(\text{vac}) - PL(\text{analyte})]/PL(\text{vac}) \quad (1)$$

**Microscopy.** Scanning electron microscopy was performed on Au-sputtered 2:1  $AgBF_4$ /PVPK films with a LEO GEMINI 1530 SEM equipped with secondary electron and backscattered electron detectors. Optical images of the films were obtained with a Nikon microscope equipped with differential interference contrast (DIC) objectives.

## RESULTS

We previously communicated that  $Ag(I)$ -impregnated luminescent polymer films, cast from either  $CH_3CN$  or THF, exhibited a proportional luminescence quenching in response to  $C_2H_4$  pressures from  $\sim 50$  Torr to saturation ca. 300 Torr.<sup>14</sup> While the linear response of these films to varying ethylene pressures was consistent between runs, the fractional quenching observed diverged. As a goal of the current study, the breadth of applicability of the gas-response paradigm was explored. In addition, microscopy studies were performed on films to explore the morphological origins of the discrepancy in fractional PL quenching observed between runs.

**Characterization of Coordination-Mediated Response.** PVPK films require the presence of  $Ag(I)$  for a response to be observed. In the absence of  $Ag(I)$ , quenching does not occur (Figure 1). Films of PVPK alone (without any

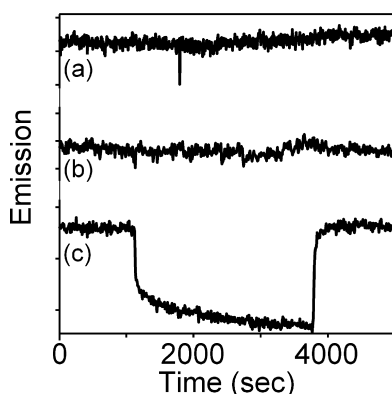


**Figure 1.**  $Ag(I)$  salts are required for polymer films to exhibit a luminescence quenching in response to  $C_2H_4$ . The change in luminescence in response to  $C_2H_4$  was plotted as a function of time for three different films cast from THF solutions: (a) PVPK, (b) 2:1  $NaBF_4$ /PVPK, and (c) 2:1  $AgBF_4$ /PVPK.

metal salt impregnation) (Figure 1a) and of PVPK impregnated with  $NaBF_4$  in a 2:1 ratio (Figure 1b) did not produce the reversible quenching that is observed upon exposure to  $C_2H_4$  with  $Ag(I)$ -impregnated films (Figure 1c and Figure S1, Supporting Information). Conditioned films of 2:1  $AgBF_4$ /PVPK respond linearly to  $C_2H_4$  exposures of varying pressures (Figure 2).

The response selectivity reveals that  $Ag(I)$ –analyte coordination is required for sensing to occur. No response was observed when a  $Ag(I)$ -impregnated PVPK film was exposed to the saturated hydrocarbon  $C_3H_8$  (Figure 3), which is incapable

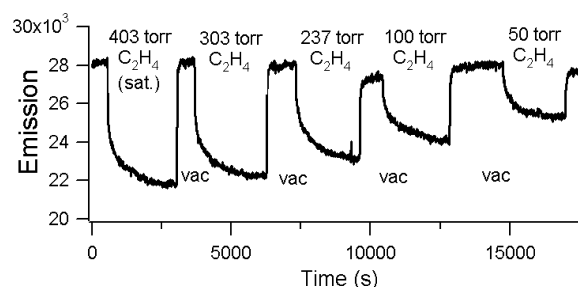


**Figure 2.** Representative plot showing PL intensity changes as a function of time that result from exposure of 2:1  $AgBF_4$ /PVPK film cast from THF to various pressures of ethylene gas. The 2:1  $AgBF_4$ /PVPK film was excited with 488 nm light, and emission was followed at 575 nm.

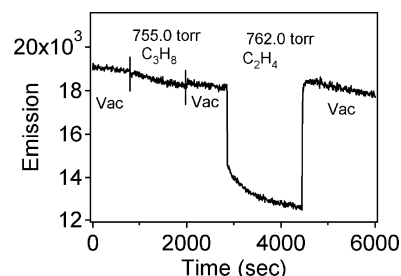


**Figure 3.** Response to saturated ( $C_3H_8$ ) and unsaturated ( $C_2H_4$ ) gaseous hydrocarbons, by a 2:1  $AgBF_4$ /PVPK film cast from THF solution, demonstrates that the film is selective for unsaturated hydrocarbons. The change in luminescence in response to the gaseous analytes (as indicated in figure) was plotted as a function of time. The film was exposed to the two analytes sequentially, and vacuum was applied between exposures. The 2:1  $AgBF_4$ /PVPK film was excited with 488 nm light, and emission was followed at 575 nm.

of coordinating to the metal centers. The response characteristics of the films were explored with a larger set of analytes: those capable of forming coordination bonds with the metal center ( $NH_3$  and  $C_3H_6$ ) induced a quenching response similar to that observed with  $C_2H_4$  (Figure 4), and those incapable of

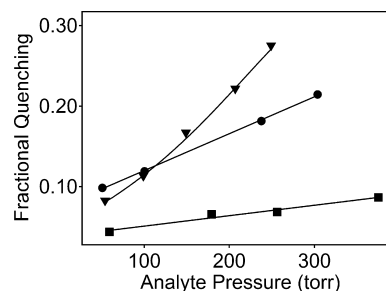


**Figure 4.**  $AgBF_4$ /PVPK (2:1) films are responsive to gaseous analytes capable of forming bonds with  $Ag(I)$ . Representative response curves for quenching of photoluminescence from THF-deposited 2:1  $AgBF_4$ /PVPK films by various analytes. Films were exposed to increasing concentrations of  $NH_3$  (■),  $C_2H_4$  (●), and  $C_3H_6$  (▼). Vacuum was applied to the films between exposures at different pressures. Fractional quenching was calculated according to eq 1.

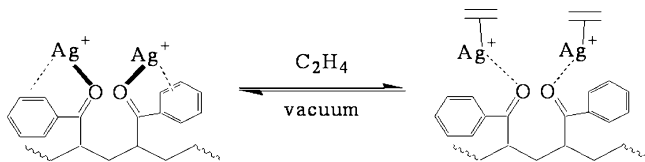
forming such bonds (i.e.,  $C_3H_8$ ,  $N_2$ , and Ar) did not induce quenching (data not shown). All analytes that induce the quenching behavior are known to coordinate to  $Ag(I)$ .<sup>30,31</sup> Emission quenching is observed for alkenes  $C_2H_4$  and  $C_3H_6$ , but the concentration dependence differs. The response curve



of  $C_3H_6$  reveals deviation from linearity toward the ordinate (Figure 4), in contrast to that of  $C_2H_4$ , which is linear. This observation suggests that the hydrophobic  $C_3H_6$  may penetrate farther into the polymer than  $C_2H_4$ , consistent with the likely greater solubility of the more hydrophobic analyte. The increased solubility may allow  $C_3H_6$  to interact with a larger proportion of the embedded Ag(I) centers and may also make the removal of  $C_3H_6$  from the films more difficult. While the films exhibit reversible quenching in response to  $NH_3$ , the magnitude of that quenching is smaller than that for either of the olefins under similar experimental conditions, presumably due to lower solubility of  $NH_3$  in the hydrophobic polymer environment.

Bonding interactions between the polymer moieties, Ag(I), and  $C_2H_4$  were investigated with IR spectroscopy<sup>14</sup> and are conceptualized in Scheme 1. We previously described the

**Scheme 1. Changes to Ag(I) Coordination Sphere upon Ethylene Exposure**



changes to the metal salt and polymer vibrations that were observed when  $AgBF_4$  was incorporated into a PVPK film, which implicate Ag(I) interaction with the polymer carbonyl and phenyl moieties.<sup>14</sup> Small changes were observed when a conditioned film impregnated with Ag(I) was exposed to  $C_2H_4$ ; notably, the phenyl  $C=C$  mode at  $1444\text{ cm}^{-1}$  decreased to a width that resembled that of neat PVPK (Figure S2, Supporting Information). The carbonyl resonance was not significantly affected by ethylene exposure (Figure S2, Supporting Information). These small changes suggest that ethylene displaces polymer phenyls from the Ag(I) coordination sphere, while carbonyl ligation is maintained. Minimal changes in the other polymer modes suggest that  $C_2H_4$  binding does not result in significant structural changes in the film.

**Factors Influencing the Observed Response.** Analyte-dependent quenching is due to vibrational relaxation, as revealed by comparison of quenching induced by equal pressures of  $C_2H_4$  and  $C_2D_4$ . The vibrational frequency of the double bond in  $C_2H_4$  ( $\nu_{C=C}$ ) decreases upon deuteration (Table 1); therefore, a smaller quenching in response to an

**Table 1. Relative Quenching Intensities of  $C_2H_4$  and  $C_2D_4$**

isotopomer	$\nu_{C=C}$ ( $\text{cm}^{-1}$ ) <sup>a</sup>	% quenching 100 Torr <sup>b</sup>	% quenching 600 Torr <sup>b</sup>
$H_2C=CH_2$	1623	14.7	20.0
$D_2C=CD_2$	1515	10.6	14.8

<sup>a</sup>Reference 50. <sup>b</sup>Percent quenching upon exposure to  $C_2X_4$  ( $X = H, D$ ) of 2:1  $AgBF_4$ /PVPK film, as calculated with eq 1.

equal pressure of the deuterated isotopomer would suggest that the response is a result of vibrational quenching upon ligation of  $C_2H_4$  to the metal center. Films of 2:1  $AgBF_4$ /PVPK were exposed to equal pressures of  $C_2H_4$  and  $C_2D_4$  in two different pressure regimes:  $\sim 100$  Torr (Figure S3, Supporting Information) and  $\sim 600$  Torr. The higher concentration was beyond the pressure required to saturate the active sites of the films. Quenching occurred upon exposure to either isotopomer;

however, the magnitude of the quenching was smaller when the films were exposed to  $C_2D_4$  (Table 1). From these results, it is concluded that analyte binding provides a nonemissive, vibrational relaxation pathway that is diminished with the heavier  $C_2D_4$ .

The strength of metal salt ion pairing affects the magnitude of the quenching upon exposure to  $C_2H_4$ . A comparison of the responses of various silver salts incorporated into PVPK films reveals a trend that mirrors the apparent strength of the ion pair. Films prepared with silver salts bearing oxygen donor anions,  $Ag(SO_3CF_3)$  and  $AgClO_4$ , which exhibit the strongest ion pairing among the salts used in this study,<sup>32,33</sup> do not respond to  $C_2H_4$  (data not shown). Films prepared with the more weakly ion-paired salts  $AgBF_4$ ,  $AgSbF_6$ , or  $AgB(C_6F_5)_4$  all respond with a luminescence quenching upon exposure to  $C_2H_4$  in a manner that is affected by the size of the paired anion (Figure 5).<sup>34,35</sup> PVPK films impregnated with  $AgBF_4$  show the

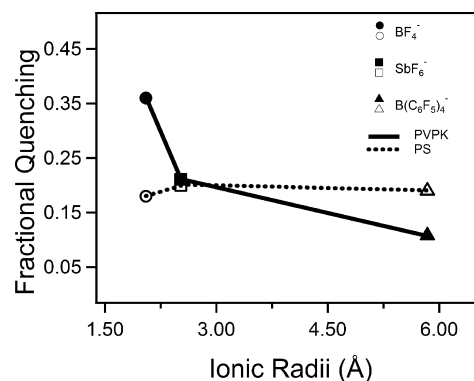


**Figure 5.** Comparison of fractional luminescence quenching demonstrated by Ag(I)-impregnated PVPK (—) and PS (---) films cast from THF as a function of the ionic radii of three silver salts:  $AgBF_4$  (●, ○),  $AgSbF_6$  (■, □), and  $AgB(C_6F_5)_4$  (▲, △). Fractional quenching data were collected upon exposure of the films to 1 atm of  $C_2H_4$ . All data are an average of the luminescence quenching values after conditioning. Fractional quenching was calculated according to eq 1.

largest fractional quenching; as the size of the counterion increases in  $AgSbF_6$  and  $AgB(C_6F_5)_4$ , the fractional quenching decreases (Table 2).

**Table 2. Fractional Quenching of a Variety of Polymer–Ag(I) Salt Matrices to  $C_2H_4$  (760 Torr)**

matrix	$AgBF_4$	$AgSbF_6$	$AgB(C_6F_5)_4$
PVPK	$0.36 \pm 0.08$	$0.21 \pm 0.07$	$0.11 \pm 0.04$
PS	$0.18 \pm 0.04$	$0.20 \pm 0.07$	$0.19 \pm 0.07$
No polymer	$0.17 \pm 0.03$	$0.17 \pm 0.06$	0.01
BMSB	$0.15 \pm 0.03$		

The film morphology is irregular, with unevenly dispersed silver salt and polymer, resulting in response variation between films of equivalent composition. Although the films consistently demonstrated fractional quenching values proportional to  $C_2H_4$  pressure, there was inconsistency in the magnitude of quenching between film preparations. When the Ag(I)-impregnated PVPK films are initially exposed to 488 nm light, a slow decrease in emission is observed; once the emission intensity has stabilized, the films are exposed to a series of  $C_2H_4$ –vacuum conditioning cycles. During these cycles, an erratic luminescence-quenching

response is demonstrated for up to six exposures of  $C_2H_4$ .<sup>14</sup> The initial exposure to  $C_2H_4$  typically results in an increase in emission. Previous IR studies revealed that during initial exposure, silver-bound solvent molecules are displaced by ethylene.<sup>14</sup> Subsequent  $C_2H_4$ -vacuum cycles during conditioning result in a lowering of the emission baseline, which may be indicative of silver-bound  $C_2H_4$  molecules that are difficult to remove. Exposure to  $C_2H_4$  for a prolonged period (ca. 2 h) during one of the conditioning cycles results in a stable background signal.

We hypothesized that these erratic responses were in part due to variations in film morphology, as has been reported for other polymer-based sensors.<sup>36</sup> The morphology of 2:1  $AgBF_4$ /PVPK films was investigated with differential interference contrast (DIC) microscopy, revealing significant heterogeneity in the film surface. Interestingly, films cast from  $CH_3CN$  (Figure 6a) and THF (Figure 6b) exhibited significant

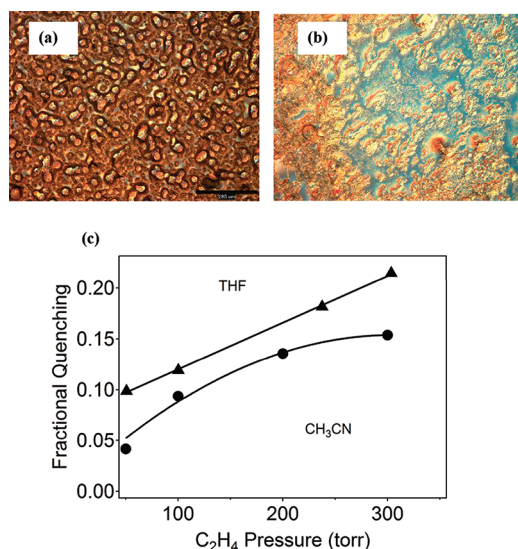


**Figure 6.** Comparison of the surface morphology and luminescence responses of films cast from  $CH_3CN$  and THF. Differential interference contrast (DIC) microscopy images of 2:1  $AgBF_4$ /PVPK films cast from (a)  $CH_3CN$  and (b) THF solutions reveal surface inhomogeneity for both. Images were obtained at 10 $\times$  magnification. (c) The response characteristics of 2:1  $AgBF_4$ /PVPK films are affected by the solvent from which they are cast. Response curves for quenching of photoluminescence from THF ( $\blacktriangle$ ) and  $CH_3CN$  ( $\bullet$ ) deposited 2:1  $AgBF_4$ /PVPK films are plotted for  $C_2H_4$  pressures of 0–300 Torr. Fractional quenching was calculated according to eq 1.

differences in their surface morphologies as revealed by the variation in color throughout the images. This difference is translated into differing response curves exhibited by 2:1  $AgBF_4$ /PVPK films cast from the two solvents:  $CH_3CN$ -cast films exhibited a response that deviated toward the abscissa, and THF-cast films exhibited a linear response (Figure 6c). The conditioning behavior of these films was also different. While  $CH_3CN$ -cast films required six conditioning cycles to displace solvent molecules bound to  $Ag(I)$  centers, THF-cast films required only one conditioning cycle.

Scanning electron micrography (SEM) revealed inhomogeneous distribution of  $Ag(I)$  within the films.  $Ag(I)$ -impregnated PVPK films deposited from THF were investigated with scanning electron microscopy (SEM) in both secondary electron mode (Figure S4a, Supporting Information) and back scattering mode (Figure S4b, Supporting Information).

Images obtained using secondary electron mode revealed surface inhomogeneity (Figure S4a, Supporting Information), as observed with DIC. Further investigation with SEM in backscattering mode revealed a high degree of electron scattering in the sample (Figure S4b, Supporting Information). Scattered electrons, present as white features in the acquired image, are produced when electrons elastically rebound from heavy atoms in a sample. The concentration of elastically scattered electrons in the SEM images is consistent with nucleation of  $AgBF_4$  within the PVPK films; homogeneous incorporation of  $Ag(I)$  throughout the polymer sample would be expected to produce a SEM image with even brightness. The combination of irregular surface morphology and heterogeneous distribution of  $Ag(I)$  in the films may be responsible for both the low percentage of sites that are quenched when films are saturated by  $C_2H_4$  and the variability in film responses. These results are consistent with the presence of accessible and inaccessible sites suggested by Stern–Volmer analysis of the response to  $C_2H_4$ .<sup>14</sup>

**Individual Contributions of the Polymer and Silver(I) Salt to the Observed Gas Response.** Given the observed salt segregation in  $Ag(I)$ –PVPK films, and the reported luminescence of  $Ag(I)$  salts,<sup>37</sup> we investigated the role of each component in the observed optical response. If  $Ag(I)$  salts independently respond to  $C_2H_4$  exposure, then the salt might be responsible for the observed emission quenching. Alternatively, if effective signal transduction to the luminescent polymer were accomplished, both components might contribute to the sensing response. In the signal transduction process, the  $Ag(I)$  ion would serve as a mediator capable of forming bonds with the polymer and the analyte. Upon exposure, the  $Ag(I)$  ion would communicate analyte binding to the polymer by altering the polymer-based emission. Experiments performed to investigate the individual role of the components include PL experiments with polymer-free silver salts, silver salts incorporated into a nonemissive support, and silver salts incorporated into the highly luminescent oligomer BMSB.

$Ag(I)$  salts luminesce in the absence of polymer support and exhibit quenching in the presence of gases; however, polymer-free silver salts are highly susceptible to photoreduction. The responses of the  $Ag(I)$  salts to  $C_2H_4$  exposure are of lower magnitude than those observed when the same salts are impregnated into PVPK (Table 2). The responses of  $AgBF_4$  or  $AgSbF_6$  proved to be short-lived with the emission quenching quickly diminishing after three or four cycles of exposure to  $C_2H_4$ . Inspection of nonresponsive  $AgBF_4$  or  $AgSbF_6$  films revealed dark spots covering the previously illuminated area of the films, which indicate photoreduction. In contrast, PVPK films impregnated with  $AgBF_4$  and  $AgSbF_6$  maintained gas responsiveness over repeated exposures, with no evidence for photoreduction within the time frame of the PL experiment (close to 5 h for the film in Figure 2). Notably,  $AgB(C_6F_5)_4$  does not respond to  $C_2H_4$  in the absence of polymer; however, in the presence of PVPK, the response from  $AgB(C_6F_5)_4$  impregnated films is of similar magnitude to the response of  $AgBF_4$  or  $AgSbF_6$  impregnated polymer films.

The polymer support promotes ion-pair separation and  $Ag(I)$  stability, preventing photoreduction. Previous IR studies with PVPK revealed the interaction of  $Ag(I)$  centers with the carbonyl and phenyl moieties of PVPK.<sup>14</sup> A nonluminescent polymer with phenyl moieties, such as PS, could serve as a stabilizing support matrix for luminescent  $Ag(I)$  salts. PS films impregnated with  $AgBF_4$  or  $AgSbF_6$  exhibit a response to  $C_2H_4$

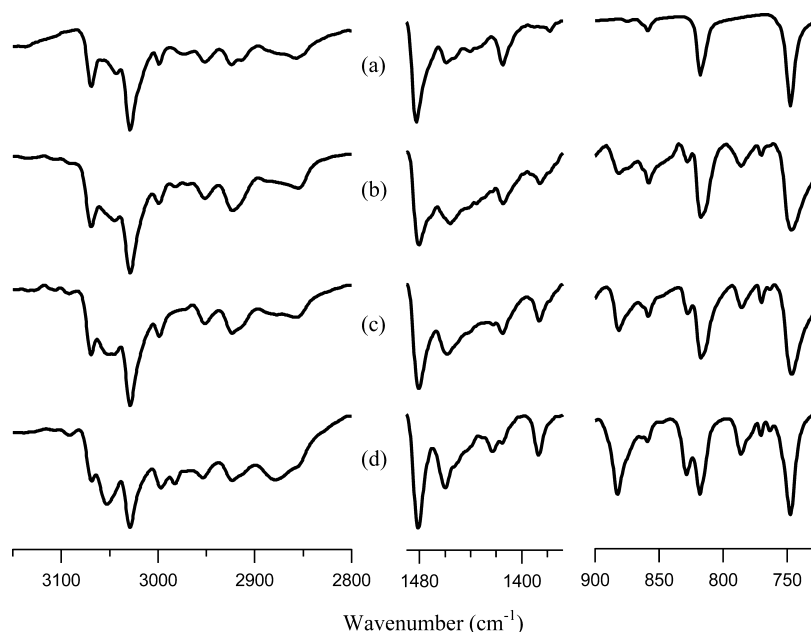


**Figure 7.** IR spectra of BMSB films impregnated with various ratios of  $\text{AgBF}_4$ . Three regions are displayed, the C–H stretch region (left), the C–C ring stretch region (middle), and the ring puckering region (right): (a) BMSB film; (b) 2:1  $\text{AgBF}_4$ /BMSB film; (c) 4:1  $\text{AgBF}_4$ /BMSB film; (d) 5:1  $\text{AgBF}_4$ /BMSB film. All films were cast from THF and placed under vacuum for an hour prior to recording the IR spectra.

at levels that are comparable to those exhibited by the salts without a support matrix (Table 2).  $\text{AgB}(\text{C}_6\text{F}_5)_4$  demonstrates a response to saturation pressures of  $\text{C}_2\text{H}_4$  when impregnated into PS, a response that is not observed for the same salt in the absence of a polymer support. This observation suggests that there is ion-pair separation within the PS support. Unlike PVPK– $\text{Ag}(\text{I})$  films, the percentage quenching exhibited by PS– $\text{Ag}(\text{I})$  films after exposure to  $\text{C}_2\text{H}_4$  is not significantly affected by counterion size (Figure 5, Table 2). Importantly, the polymer support provides stability to the  $\text{Ag}(\text{I})$  ions, which allows PS films impregnated with  $\text{Ag}(\text{I})$  salts to exhibit a reproducible luminescence quenching upon repeated  $\text{C}_2\text{H}_4$  exposures.

The preceding PL experiments established that polymer-free and polymer-supported  $\text{Ag}(\text{I})$  salts respond to ethylene exposure with an emission quenching; however, communication of the ethylene binding event at the  $\text{Ag}(\text{I})$  ions to the supporting matrix was not demonstrated. Experimental conditions contribute to uncertainty in whether the  $\text{Ag}(\text{I})$  ions or the supporting PVPK matrix generates the response signal. Since PVPK undergoes Norrish type II photodegradation upon excitation with 360 nm light,<sup>38</sup> the films are excited at the tail end of the film absorption, at 488 nm. The species that comprise the end of the absorption spectrum do not exhibit bulk film behavior and therefore are likely to have unique coordination environments and produce uncharacteristic emission spectra not firmly distinguishable from those of the silver salts.

**Demonstration of Coordination-Mediated Signal Transduction.** Additional PL experiments with silver impregnated films of the well-characterized luminescent oligomer BMSB are a logical way to test transduction of the gas-binding signal to the support. BMSB is a highly luminescent  $\pi$ -conjugated oligomer that was previously shown to form  $\text{Ag}(\text{I})$  coordination polymers with a distinctive absorption band ( $\pi \rightarrow \pi^*$  transition) centered at 445 nm.<sup>39</sup> Excitation of this transition produces an intense emission band centered at 488 nm, easily distinguishable from bands of the weakly emissive  $\text{Ag}(\text{I})$  salts. Significant changes in the emission intensity of this band upon exposure of a BMSB/ $\text{AgBF}_4$

film to  $\text{C}_2\text{H}_4$  would be attributable to  $\text{Ag}(\text{I})$ -mediated gas-binding signal transduction.

IR spectroscopy reveals direct interaction between the metal salt and the oligomer in  $\text{AgBF}_4$ /BMSB films. Three regions of the BMSB IR spectrum provide significant information: (1) 725–900  $\text{cm}^{-1}$ , a region that displays ring puckering stretches and C–H wags (ca. 747, 818, and 875  $\text{cm}^{-1}$ ),<sup>40,41</sup> (2) 1350–1490  $\text{cm}^{-1}$ , the C–C ring stretch region (ca. 1378 and 1414  $\text{cm}^{-1}$ ),<sup>40,41</sup> and (3) 2800–3150  $\text{cm}^{-1}$ , a region that contains aromatic and aliphatic C–H stretches (ca. 2850  $\text{cm}^{-1}$ ).<sup>40,41</sup> IR spectra of these regions are displayed in Figure 7. BMSB also displays strong bands at 963 and 974  $\text{cm}^{-1}$  associated with C–H wags of the vinylene groups (not shown).<sup>42</sup> Incorporation of  $\text{AgBF}_4$  into BMSB results in significant changes to the oligomer vibrations. For example, the addition of 2 equiv of  $\text{AgBF}_4$  results in the appearance of an additional trio of peaks in the C–H wag and ring puckering region at 783, 832, and 883  $\text{cm}^{-1}$  (Figure 7b). These peaks, not observed in the  $\text{AgBF}_4$  spectrum, are presumably related to the BMSB peaks at 747, 818, and 875  $\text{cm}^{-1}$ , and indicate an interaction of the BMSB phenyl rings with the metal centers. In the C–C ring stretch region, additional peaks appear at 1385 and 1422  $\text{cm}^{-1}$ , near the BMSB peaks at 1378 and 1414  $\text{cm}^{-1}$ . The oligomer C–H stretches are also affected by  $\text{Ag}(\text{I})$  incorporation, with a shift of an aliphatic C–H stretch mode moving from 2850  $\text{cm}^{-1}$  to 2860  $\text{cm}^{-1}$ . Broadening of the aromatic C–H stretches is also observed. Changes to the C–H wags associated with the oligomer vinylene groups are not easily observed, since these stretches overlap with the broad  $\text{BF}_4^- \nu_3$  mode centered at 1065  $\text{cm}^{-1}$ .

The optimal  $\text{Ag}(\text{I})$ /BMSB ratio was determined by following the effect of varied  $\text{Ag}(\text{I})$  salt concentration on the BMSB oligomer vibrations. Increasing the  $\text{AgBF}_4$ /BMSB ratio results in further  $\text{Ag}(\text{I})$  coordination to the oligomer, with newly observed peaks at 783, 832, and 883  $\text{cm}^{-1}$  that increase in intensity as 4 and 5 equiv of  $\text{Ag}(\text{I})$  are incorporated into BMSB (Figure 7c,d). A sharpening of the BMSB peaks at 747 and 818  $\text{cm}^{-1}$  is also observed (Figure 7d), with the width of those



peaks comparable to that of the neat BMSB film. This peak sharpening suggests a more homogeneous coordination environment for the oligomer aromatic rings. Concurrently, aromatic C–C stretches at 1385 and 1422  $\text{cm}^{-1}$  and an aliphatic C–H stretch at 2860  $\text{cm}^{-1}$  overshadow in intensity the related BMSB peaks at 1378, 1415, and 2850  $\text{cm}^{-1}$ , respectively. Also, a sharp peak centered at 3050  $\text{cm}^{-1}$  appears in the aromatic C–H region. Interaction between BMSB and the metal salts maximizes at a 5:1 ratio; thereafter, increasing the Ag(I) equiv reduces the relative intensity of the newly observed peaks, possibly due to salt aggregation. Together, these data suggest that the optimal Ag(I)/BMSB ratio for PL experiments to be 5:1.

Silver(I) ions modulate changes in emission of the highly luminescent BMSB oligomer upon ethylene binding. Films of the luminescent oligomer BMSB impregnated with 5 equiv of  $\text{AgBF}_4$  salt exhibit a strong  $\pi \rightarrow \pi^*$  transition band centered at 438 nm. This band closely matches the  $\pi \rightarrow \pi^*$  transition centered at 445 nm previously observed for the  $\text{AgBF}_4$ /BMSB coordination polymer.<sup>39</sup> The films exhibited an intense emission band at 482 nm upon excitation of the  $\pi \rightarrow \pi^*$  transition. The observed emission is oligomer-based, because no emission was registered when a neat  $\text{AgBF}_4$  film was excited under similar experimental conditions. The 5:1  $\text{AgBF}_4$ /BMSB films respond to  $\text{C}_2\text{H}_4$  exposure with a reversible decrease in emission intensity (Figure S5, Supporting Information). There was no emission change when films of BMSB alone were exposed to  $\text{C}_2\text{H}_4$  (not shown) or when the Ag(I)-impregnated films were exposed to air (not shown) or  $\text{C}_2\text{H}_6$  (Figure S5, Supporting Information). Films of 5:1  $\text{AgSbF}_6$ /BMSB respond with irreversible quenching to CO exposure; the IR spectrum reveals three  $\nu_{\text{CO}}$  modes at 2137, 2083, and 2023  $\text{cm}^{-1}$  (Figure S6, Supporting Information). While the mode at 2137  $\text{cm}^{-1}$  is indicative of CO trapped within the polymer matrix, the modes at 2083 and 2023  $\text{cm}^{-1}$  suggest the presence of metal-bound CO species. Direct observation of metal-bound CO suggests that it is irreversible binding of CO to the Ag(I) ions that is responsible for the irreversible quenching. After one conditioning cycle, impregnated films respond in a proportional manner to  $\text{C}_2\text{H}_4$  pressures between  $\sim 50$  and  $\sim 400$  Torr. Film conditioning also results in the emergence of a stable background signal between ethylene exposures. A representative PL plot of a 5:1  $\text{AgBF}_4$ /BMSB film is shown in Figure S7, Supporting Information. Exposure to an atmosphere of ethylene results in an emission quenching of comparable percentage to those of  $\text{AgBF}_4$ /PS films (Table 2). Stern–Volmer analysis (Figure 8) of the response of Ag(I)-doped BMSB films reveals a plot in which the ordinate deviates toward the abscissa, as was observed in 2:1  $\text{AgBF}_4$ /PVPK films cast from acetonitrile. This deviation is indicative of inaccessible binding sites within the films, which cannot be quenched by ethylene. The modified Stern–Volmer plot (Figure 8, inset) implies that  $17.9\% \pm 2.8\%$  of the sites are accessible to ethylene quenching. Together, these data demonstrate an effective gas-sensing transduction from the silver salts to the luminescent oligomer support. The strong similarity between PL experiments of Ag(I)-impregnated BMSB and PVPK films suggests that the luminescent support also contributes to the gas-sensing response observed with impregnated PVPK films.

## DISCUSSION

Both the Ag(I) salt and the polymer (or oligomer) play separate and significant roles in sensing of gaseous analytes by

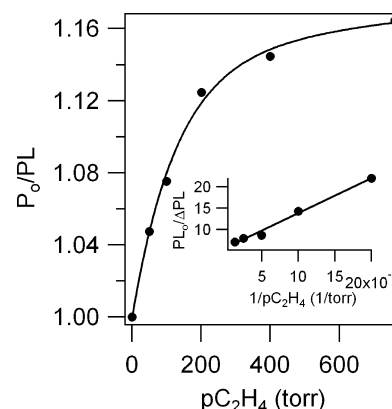


**Figure 8.** Stern–Volmer analysis of PL data from a 5:1  $\text{AgBF}_4$ /BMSB film (data shown in Figure S5, Supporting Information) with line of best fit ( $\chi^2 = 6.95 \times 10^{-5}$ ). Note the deviation of the curve toward the abscissa, an indication of sites in the film accessible and inaccessible to ethylene. The modified Stern–Volmer plot (inset) reveals that only  $17.9(\pm 2.8)\%$  of the luminescent available sites are quenched by ethylene. Analysis of the slope reveals that the binding constant is  $K_{\text{sv}} = (6.78 \pm 2.15) \times 10^{-3} \text{ Torr}^{-1}$ .

Ag(I)-impregnated films. Proportional quenching responses were observed only with analytes that bind coordinately to Ag(I), indicating that the Ag(I) centers serve to transduce the gas-binding signal through ligand binding. The polymer (or oligomer) support also contributes to sensing: it activates the Ag(I) salt by inducing ion-pair separation, mitigates photo-degradation of the Ag(I) ion, and, when luminescent, serves as reporter through its emission. The Ag(I) salts tested fall into two general categories: those with fluorine-rich anions that become ion-pair separated upon impregnation and may transduce the gas-binding signal and those with oxygen-rich anions that are ineffective as signal transducers. The behaviors that we observe in this sensing application are consistent with those previously noted when Ag(I)-impregnated polymers were used in facilitated transport.

The effect of ion-pair separation on Ag(I)–olefin complex formation has been established in facilitated transport applications. Ag(I)-impregnated polymer membranes separate olefins (alkenes) from paraffins (alkanes) in petroleum gas mixtures by using Ag(I)–olefin interactions to promote olefin transfer through the membrane.<sup>43,44</sup> The strength of ion pairing in the Ag(I) salts has been identified as a significant factor in the accessibility of Ag(I) to olefins and a prime determinant of the efficacy of these films.<sup>45,46</sup> Ag(I) salts with larger anions form more stable complexes with olefins, which generally correlate with improved performance of facilitated transport films impregnated with these salts.<sup>33</sup> Further, the exposed Ag(I) cations form cross-links with the polymer, increasing the olefin permeability and efficacy in facilitated transport. By analogy, increased olefin permeability in the sensor films should result in an increase in the number of Ag(I) centers that encounter  $\text{C}_2\text{H}_4$ .

The polymers and oligomer used in this study aid in ion-pair separation, thus enhancing the sensing behavior of active silver salts. A comparison of the quenching response of  $\text{AgBF}_4$  on its own and when the salt is impregnated in a polymer illustrates this point.  $\text{AgBF}_4$ , which has a relatively open crystal scaffold and low lattice energy,<sup>47</sup> exhibits a greater emission quenching when impregnated in films than when it lacks a support. In a crystallographic study of  $(p\text{-methylacetophenone})_2\text{AgBF}_4$ ,<sup>48</sup>

which is a reasonable model for  $\text{AgBF}_4$  in PVPK,  $\text{BF}_4^-$  was completely displaced from  $\text{Ag(I)}$  and the coordination sphere of the metal was filled by two phenyl rings and two carbonyl groups. A similar ion-separated environment for  $\text{Ag(I)}$  may be present in  $\text{Ag(I)}$ -impregnated PVPK; coordination of  $\text{Ag(I)}$  to the carbonyl groups and phenyl rings was indeed implicated in our prior IR studies.<sup>14</sup> A coordination polymer of  $\text{AgBF}_4$  and BMSB was crystallographically characterized, and again the  $\text{BF}_4^-$  anion was not bound to the  $\text{Ag(I)}$  ion.<sup>39</sup> In this polymer, the coordination environment of the  $\text{Ag(I)}$  was filled by two phenyl rings from two different BMSB oligomers, with each phenyl ring coordinated in an  $\eta^2$  fashion. We infer that in our films BMSB and PS may interact with  $\text{Ag(I)}$  in a similar fashion. Consistent with these conclusions, we observed that  $\text{AgBF}_4$  gave rise to ethylene-induced quenching in all the films tested, presumably due to effective ion-pair separation that occurs upon impregnation in the coordinating films. The larger quenching for  $\text{AgBF}_4$  upon incorporation in PVPK, as opposed to BMSB or PS, is likely due to the greater ability of PVPK to induce ion-pair separation through interactions with both carbonyl and phenyl moieties, as opposed to interaction only with the phenyl moieties of PS or BMSB.

Ion-pair separation plays an even more extensive role in the behavior of  $\text{AgB(C}_6\text{F}_5)_4$ .  $\text{AgB(C}_6\text{F}_5)_4$  does not respond to  $\text{C}_2\text{H}_4$  in the absence of a polymer support, which may be attributed to coordinative interactions with the anion that inhibit interaction of  $\text{Ag(I)}$  with  $\text{C}_2\text{H}_4$ . A crystal structure of  $\text{AgBF}_4$  grown from deuterobenzene revealed that  $\text{Ag(I)}$  binds a single fluorine and up to three separate deuterobenzene molecules in either an  $\eta^1$  or  $\eta^2$  mode.<sup>49</sup> This crystal structure suggests that in the films  $\text{C}_6\text{F}_5$  moieties of the  $\text{B(C}_6\text{F}_5)_4^-$  anion may preferentially bind to the  $\text{Ag(I)}$  center, rendering it coordinatively saturated and preventing it from interacting with  $\text{C}_2\text{H}_4$ .  $\text{AgB(C}_6\text{F}_5)_4$  demonstrates sensory behavior in the presence of PS or PVPK and is the only salt that demonstrates a larger quenching when impregnated in PS than when impregnated in PVPK. PS is less polar than PVPK and its phenyl moiety may interact to a greater extent with the  $\text{C}_6\text{F}_5$  moiety of  $\text{B(C}_6\text{F}_5)_4^-$ , thus promoting more effective ion-pair separation in  $\text{AgB(C}_6\text{F}_5)_4$ .

Although polymer impregnation activates  $\text{AgB(C}_6\text{F}_5)_4$ , not all  $\text{Ag(I)}$ -polymer interactions improve the sensory response characteristics of the polymer films. The behavior of  $\text{AgSbF}_6$  and  $\text{AgSbF}_6$ -impregnated PVPK in response to  $\text{C}_2\text{H}_4$  illustrates this point. Room-temperature emission from  $\text{AgSbF}_6$  in the absence of polymer support has been previously studied.<sup>37</sup> We observed that the  $\text{C}_2\text{H}_4$ -induced fractional quenching exhibited by  $\text{AgSbF}_6$  in the absence of a polymer was larger than that in the presence of a polymer support. This difference may be plausibly explained by phase separation and emission from pure PVPK regions that cannot be quenched. That is, those polymer moieties that are not interacting with  $\text{AgSbF}_6$  may provide a baseline emission that interferes with luminescence quenching from potentially active regions of the film.

Counterion size influences the efficacy of ion-pair separation in the presence of PVPK. As one moves from  $\text{BF}_4^-$  to the larger counterions  $\text{SbF}_6^-$  and  $\text{AgB(C}_6\text{F}_5)_4^-$ , there is a decrease in the quenching intensity of the impregnated PVPK films. This observation seems inconsistent with the greater ion-pair separation expected for  $\text{SbF}_6^-$  and  $\text{AgB(C}_6\text{F}_5)_4^-$ ; however, this effect may reflect the formation of difficult-to-disrupt  $\text{Ag(I)}$ - $\text{C}_2\text{H}_4$  complexes during film conditioning. If  $\text{B(C}_6\text{F}_5)_4^-$  and  $\text{SbF}_6^-$ , when incorporated into PVPK, achieve greater separation

from the  $\text{Ag(I)}$  ion than  $\text{BF}_4^-$ , then these salts are more likely to form  $\text{Ag(I)}$ - $\text{C}_2\text{H}_4$  complexes that are resistant to removal by exposure to vacuum. The formation of such resistant complexes would reduce the quenching efficacy of the films, consistent with a decrease in the background signal observed during film conditioning. Together, these observations reveal the multifaceted role ion-pair separation plays in the quenching efficacy of the films. Effective ion-pair separation, a result of strong  $\text{Ag(I)}$  salt interaction with the polymer support, grants to impregnated PVPK films greater  $\text{Ag(I)}$  ion stability and quenching efficacy upon ethylene exposure than is characteristic of the bare  $\text{Ag(I)}$  salts. However, these effects must be balanced against formation of stable  $\text{Ag(I)}$ - $\text{C}_2\text{H}_4$  complexes that reduce the reversibility and magnitude of the gas-sensing response.

$\text{Ag(I)}$  salts with oxygen-rich counterions do not sensitize films for gas sensing because ion-pair separation does not occur. Sensor films impregnated with  $\text{Ag(I)}$  salts with the oxygen-rich counterions  $\text{AgClO}_4$  and  $\text{Ag(CF}_3\text{SO}_3)$  do not respond to ethylene, supporting the idea that there is competition between the counterion and analyte for the  $\text{Ag(I)}$  center. Presumably in these salts the  $\text{Ag(I)}$ -counterion interaction is too strong to be disrupted upon incorporation into the polymer matrix. Although  $\text{AgBF}_4$  or  $\text{AgClO}_4$  both bind to olefins in the absence of polymer,<sup>32</sup> the behavior of these salts in polymer films is differentiated by the effect of the anion on the  $\text{Ag(I)}$  coordination environment. In the case of BMSB and a closely related oligomer,  $\text{AgClO}_4$  and  $\text{Ag(CF}_3\text{SO}_3)$  formed coordination polymers in which the counterion remained coordinately bound to the metal ion.<sup>39</sup> In facilitated transport,  $\text{Ag(I)}$  salts with oxygen donor anions did not perform as well as those with fluorinated counterions; the difference was attributed to tighter ion pairing between oxygen donor anions and  $\text{Ag(I)}$  than with fluorinated anions.<sup>32</sup> Despite the similarity and lattice energy of  $\text{AgClO}_4$  and  $\text{AgBF}_4$ , there was a significant difference in olefin permeability of poly(2-ethyl-2-oxazoline) when impregnated with these salts.<sup>33</sup> The poorer performance of the  $\text{AgClO}_4$ -impregnated polymer was attributed to strong interaction between the anion and cation, which interferes with  $\text{Ag(I)}$ - $\text{C}_2\text{H}_4$  complex formation and reduces the ability of  $\text{Ag(I)}$  to form transient cross-links to open the polymer geometry. A vibrational spectroscopic study of the interaction of  $\text{Ag(I)}$  with the polymer functional groups and with the counterions indicated that ion pairing was weaker in  $\text{AgBF}_4$ -impregnated films than in  $\text{AgClO}_4$ -impregnated ones.<sup>32</sup> The poor performance of  $\text{AgClO}_4$ -impregnated facilitated transport films is thus consistent with the lack of response observed with the sensor films.

Irregular film morphology on the gross scale may cause significant variation in  $\text{Ag(I)}$  salt-polymer interactions, requiring that the films be conditioned to become active. The heterogeneous morphology of the films suggests the polymer may contain  $\text{Ag(I)}$  sites with varying stability. Those less stable sites are reduced during conditioning; the photoreduction would contribute to the loss of luminescence from the films upon initial exposure to the light source. Similar behavior has been exhibited by facilitated transport films, where exposure to UV irradiation has also been shown to result in photoreduction of  $\text{Ag(I)}$ . Difficult to remove  $\text{Ag(I)}$ - $\text{C}_2\text{H}_4$  complexes also form during conditioning. These complexes partly account for the irreversible reduction in the emission baseline observed during film conditioning. That the conditioned films are able to maintain a consistent baseline during these experiments



suggests that the polymer is capable of maintaining the viability of the remaining Ag(I) in the active sensor films.

Irregular Ag(I) salt–polymer interactions due to irregular morphology also lead to significant variation in luminescence quenching intensities in response to equal pressures of analytes. Our studies revealed that approximately 20% of the Ag(I) sites are involved in the quenching event and that less than 50% of the luminescence is quenched in any of the films upon exposure to 760 Torr  $C_2H_4$ .<sup>14</sup> Although the films consistently demonstrate proportional sensing behavior, the response characteristics (i.e., luminescence and quenching intensities) varied between films, behavior that is consistent with other sensors that rely on polymer-based interfaces.<sup>36</sup> Since Ag(I) salts are unevenly distributed within films of PVPK, we infer that portions of PVPK that are not in contact with Ag(I) are inert for sensing. Furthermore, the film morphology was dependent on the deposition solvent, and the response characteristics (i.e., linear vs curved responses) of the films appeared to correlate with their differing surface morphologies. While the sensing paradigm presented herein was effective in detecting varying pressures of ethylene, the sensitivity achieved is orders of magnitude below the levels of ethylene maintained in produce storage (1 ppm) or ripening facilities (as low as 10 ppm). Since the film morphology appears to influence the accessibility of Ag(I) salts to  $C_2H_4$ , greater control of film morphology might improve the sensitivity of this simple gas sensor.

## CONCLUSIONS

We have demonstrated that Ag(I)-impregnated films are selective for gaseous analytes that can form bonds with the Ag(I) center and are unresponsive to those that cannot. The response is observed as a luminescence quenching, which occurs through vibrational relaxation upon interaction of the analyte with Ag(I). Both components, the Ag(I) salt and luminescent support, contribute to the quenching response observed. Polymer films do not exhibit any response to gaseous analytes in the absence of the metal salt. While Ag(I)-impregnated BMSB films selectively respond to gaseous analytes that can form bonds with the Ag(I) center, the response is purely oligomer-based and confirms signal transduction to the luminescent support from the metal salt in this sensing paradigm. In addition to serving as support for Ag(I) salts and as a recipient of their sensing signal, the oligomer/polymer affects the response characteristics of the salts by separating the Ag(I) from its anion and facilitating the accessibility of Ag(I) to the gaseous analytes. Optimization of this sensing paradigm could potentially allow the widespread use of metal-impregnated luminescent polymers or oligomers as gas sensors.

## ASSOCIATED CONTENT

### Supporting Information

Figures showing emission spectra and SEM images of 2:1  $AgBF_4$ /PVPK films, quenching response of 2:1  $AgBF_4$ /PVPK films to  $C_2H_4$  and  $C_2D_4$ , IR spectra of 2:1  $AgBF_4$ /PVPK films exposed to  $C_2H_4$ , IR spectra of 5:1  $AgBF_4$ /BMSB films exposed to  $CO$ , and the selective quenching response of 5:1  $AgBF_4$ /BMSB films to  $C_2H_4$ . This material is available free of charge via the Internet at <http://pubs.acs.org>.

## AUTHOR INFORMATION

### Corresponding Author

\*Tel: 608-262-0328. Fax: 608-262-6143. E-mail: [burstyn@chem.wisc.edu](mailto:burstyn@chem.wisc.edu)

### Present Address

<sup>‡</sup>Currently at the Southern Regional Research Center, U.S. Department of Agriculture.

## ACKNOWLEDGMENTS

The authors thank the ACS-PRF (Grant No. 42041-AC3 to J.N.B.) and the Kirchstein NRSA predoctoral fellowship (NIGMS Grant No. GM070440 to M.S.C.) for funding. This work is partially supported by the Materials Science Center and the College of Engineering of the University of Wisconsin—Madison, who provided the instrumentation used to collect data included herein. Any opinions, findings, conclusions or recommendations expressed in this paper are those of the authors and do not reflect the views of the Materials Science Center, the College of Engineering, or the University of Wisconsin—Madison. The study presented here is based in part upon work by M.S.C. while serving at and supported by the United States Department of Agriculture. The use of a company or product name is solely for the purpose of providing specific information and does not imply approval or recommendation by the United States Department of Agriculture to the exclusion of others.

## REFERENCES

- (1) Abeles, F. B.; Morgan, P. W.; Saltveit, M. E., Jr. *Ethylene in Plant Biology*, 2nd ed.; Academic Press: San Diego, CA, 1992; pp 1, 17–19, 285–296.
- (2) Chang, C.; Bleecker, A. B. *Plant Physiol.* **2004**, *136*, 2895–2899.
- (3) Rodríguez, F. I.; Esch, J. J.; Hall, A. E.; Binder, B. M.; Schaller, G. E.; Bleecker, A. B. *Science* **1999**, *283*, 996–998.
- (4) Wang, K. L.-C.; Li, H.; Ecker, J. R. *Plant Cell* **2002**, *14*, S131–151.
- (5) Beyer, E. M. Jr. *Plant Physiol.* **1976**, *58*, 268–271.
- (6) Feng, X.; Apelbaum, A.; Sisler, E. C.; Goren, R. *Postharvest Biol. Technol.* **2000**, *20*, 143–150.
- (7) Sisler, E. C.; Shang, F. Y. *Phytochemistry* **1984**, *23*, 2765–2768.
- (8) Wills, R. B. H.; Warton, M. A.; Ku, V. V. *Aust. J. Exp. Agric.* **2000**, *40*, 465–470.
- (9) Sakai, S. U.S. Patent 4,535,315, 1985.
- (10) Scotoni, M.; Rossi, A.; Bassi, D.; Buffa, R.; Iannotta, S.; Boschetti, A. *Appl. Phys. B: Lasers Opt.* **2006**, *82*, 495–500.
- (11) Pham-Tuan, H.; Vercammen, J.; Devos, C.; Sandra, P. *J. Chromatogr., A* **2000**, *868*, 249–259.
- (12) Sirisuk, A.; Hill, C. G.; Anderson, M. A. *Catal. Today* **1999**, *54*, 159–164.
- (13) Esser, B.; Swager, T. M. *Angew. Chem., Int. Ed.* **2010**, *49*, 8872–8875.
- (14) Green, O.; Smith, N. A.; Ellis, A. B.; Burstyn, J. N. *J. Am. Chem. Soc.* **2004**, *126*, 5952–5953.
- (15) Azhin, M.; Kaghazchi, T.; Rahmani, M. *J. Ind. Eng. Chem.* **2008**, *14*, 622–638.
- (16) Zilversmit, D. B. *Science* **1965**, *149*, 874–876.
- (17) Ward, W. J.; Robb, W. L. *Science* **1967**, *156*, 1481–1484.
- (18) Eriksen, O. I.; Aksnes, E.; Dahl, I. M. *J. Membr. Sci.* **1993**, *85*, 89–97.
- (19) LeBlanc, O. H. Jr.; Ward, W. J.; Matson, S. L.; Kimura, S. G. *J. Membr. Sci.* **1980**, *6*, 339–343.
- (20) Kim, Y. H.; Ryu, J. H.; Bae, J. Y.; Kang, Y. S.; Kim, H. S. *Chem. Commun.* **2000**, 195–196.
- (21) Lin, Y. S.; Ji, W.; Wang, Y.; Higgins, R. J. *Ind. Eng. Chem. Res.* **1999**, *38*, 2292–2298.
- (22) Riggs, J. A.; Smith, B. D. *J. Am. Chem. Soc.* **1997**, *119*, 2765–2766.
- (23) Steigelmann, E. F.; Hughes, R. D. U.S. Patent 3,758,603, 1973.
- (24) Koval, C. A.; Spontarelli, T. *J. Am. Chem. Soc.* **1988**, *110*, 293–295.

- (25) Kang, Y. S.; Kim, J. H.; Won, J.; Kim, H. S., Solid-State Facilitated Transport Membranes for Separation of Olefins/Paraffins and Oxygen/Nitrogen. In *Materials Science of Membranes for Gas and Vapor Separation*; Yampolskii, Y., Pinnau, I., Freeman, B., Eds.; John Wiley & Sons, Ltd.: Chichester, England, 2006; pp 391–410.
- (26) Jose, B.; Ryu, J. H.; Kim, Y. J.; Kim, H.; Kang, Y. S.; Lee, S. D.; Kim, H. S. *Chem. Mater.* **2002**, *14*, 2134–2139.
- (27) Pinnau, I.; Toy, L. G. *J. Membr. Sci.* **2001**, *184*, 39–48.
- (28) Heyns, K.; Paulsen, H. *Angew. Chem.* **1960**, *72*, 349–349.
- (29) Hayashi, Y.; Rohde, J. J.; Corey, E. J. *J. Am. Chem. Soc.* **1996**, *118*, 5502–5503.
- (30) Cotton, F. A. W., G.; Murillo, C. A.; Bochmann, M. *Advanced Inorganic Chemistry*, 6th ed.; John Wiley and Sons, Inc: New York, 1999; p 1093.
- (31) Ziegler, T.; Rauk, A. *Inorg. Chem.* **1979**, *18*, 1558–1565.
- (32) Kim, J. H.; Min, B. R.; Kim, C. K.; Won, J.; Kang, Y. S. *J. Phys. Chem. B* **2002**, *106*, 2786–2790.
- (33) Kim, J. H.; Min, B. R.; Kim, C. K.; Won, J.; Kang, Y. S. *Macromolecules* **2001**, *34*, 6052–6055.
- (34) LeSuer, R. J.; Buttolph, C.; Geiger, W. E. *Anal. Chem.* **2004**, *76*, 6395–6401.
- (35) Roobottom, H. K.; Jenkins, H. D. B.; Passmore, J.; Glasser, L. *J. Chem. Educ.* **1999**, *76*, 1570–1573.
- (36) Rajakovic, L. V.; Strbac, S. *Anal. Chim. Acta* **1995**, *315*, 83–91.
- (37) Kunkely, H.; Vogler, A. *Inorg. Chem. Commun.* **2004**, *7*, 400–401.
- (38) Golemba, F. J.; Guillet, J. E. *Macromolecules* **1972**, *5*, 212–216.
- (39) Liu, S. Q.; Kuroda-Sowa, T.; Konaka, H.; Suenaga, Y.; Maekawa, M.; Mizutani, T.; Ning, G. L.; Munakata, M. *Inorg. Chem.* **2005**, *44*, 1031–1036.
- (40) Choi, C. H.; Kertesz, M. *J. Phys. Chem. A* **1997**, *101*, 3823–3831.
- (41) Watanabe, H.; Okamoto, Y.; Furuya, K.; Sakamoto, A.; Tasumi, M. *J. Phys. Chem. A* **2002**, *106*, 3318–3324.
- (42) Sakamoto, A.; Furukawa, Y.; Tasumi, M. *J. Phys. Chem.* **1992**, *96*, 1490–1494.
- (43) Antonio, M. R.; Tsou, D. T. *Ind. Eng. Chem. Res.* **1993**, *32*, 273–278.
- (44) Sunderrajan, S.; Freeman, B. D.; Hall, C. K. *Ind. Eng. Chem. Res.* **1999**, *38*, 4051–4059.
- (45) Quinn, H. W.; Glew, D. N. *Can. J. Chem.* **1962**, *40*, 1103–1112.
- (46) Lee, D. H.; Kang, Y. S.; Kim, J. H. *Macromol. Res.* **2009**, *17*, 104–109.
- (47) Kim, C. K.; Won, J.; Kim, H. S.; Kang, Y. S.; Li, H. G.; Kim, C. K. *J. Comput. Chem.* **2001**, *22*, 827–834.
- (48) Crist, D. R.; Hsieh, Z. H.; Quicksall, C. O.; Sun, M. K. *J. Org. Chem.* **1984**, *49*, 2478–2483.
- (49) Batsanov, A. S.; Crabtree, S. P.; Howard, J. A. K.; Lehmann, C. W.; Kilner, M. J. *Organomet. Chem.* **1998**, *550*, 59–61.
- (50) Harris, D. C.; Bertolucci, M. D. *Symmetry and Spectroscopy: An Introduction to Vibrational and Electronic Spectroscopy*; Dover Publications, Inc.: New York, 1978; p 592.